Electronic Supplementary Material (ESI) for Journal of Materials Chemistry A.

Supporting information:

15% efficient carbon based planar-heterojunction perovskite solar cells using TiO_2/SnO_2 bilayer as electron transport layer

Zhiyong Liu, Bo Sun, Xingyue Liu, Jinghui Han, Haibo Ye, Yuxue Tu, Chen Chen, Tielin Shi, Zirong Tang and Guanglan Liao*

State Key Laboratory of Digital Manufacturing Equipment and Technology, Huazhong University of Science and Technology, Wuhan 430074, China.

** Address correspondence to (G. Liao) guanglan.liao@hust.edu.cn.*

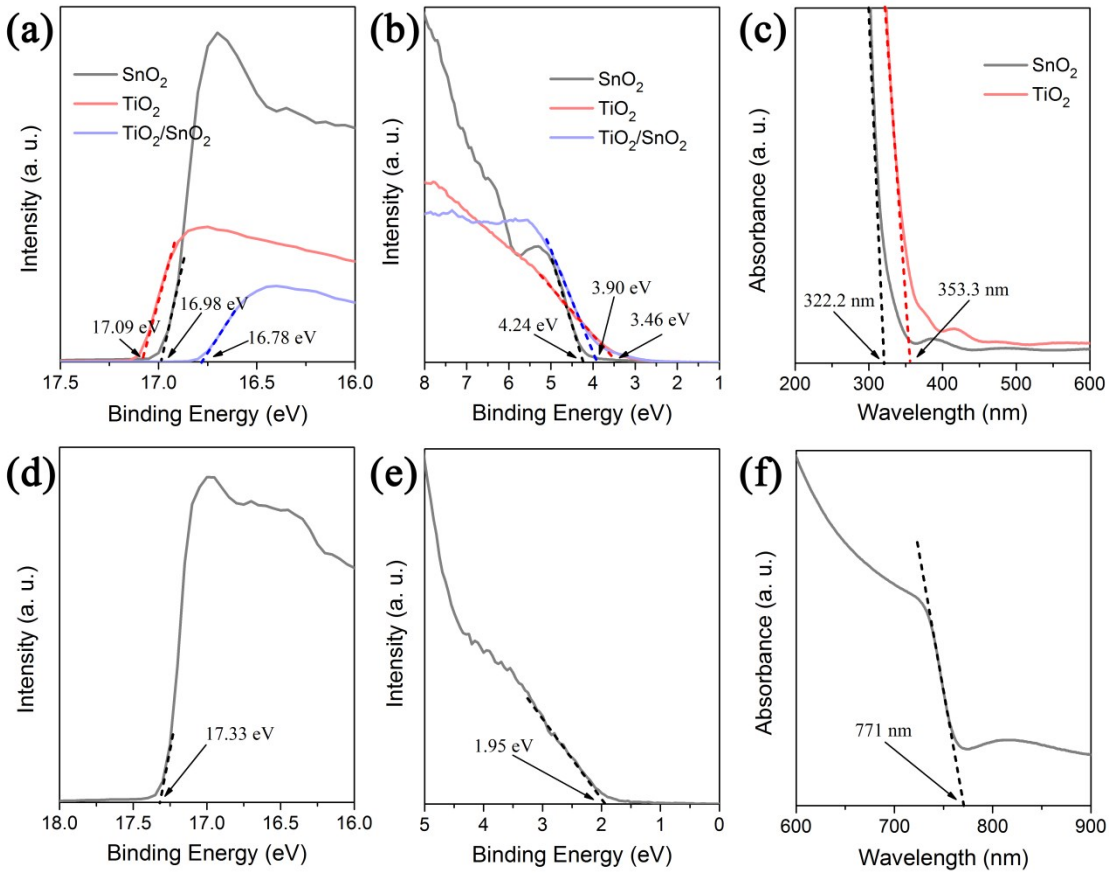

Fig. S1 (a) UPS spectra at the cutoff (E_{cutoff}) energy regions of SnO_2, TiO_2 and TiO_2/SnO_2 films. The obtained Fermi levels (Φ) for SnO_2, TiO_2 and TiO_2/SnO_2 films are 4.23 eV, 4.12 eV and 4.43 eV, respectively. (b) The energy gaps between the Fermi level with the valence band (E_f-E_v) for SnO_2, TiO_2 and TiO_2/SnO_2 films are 4.24 eV, 3.46 eV and 3.90 eV. (c) The absorption edges of SnO_2 and TiO_2 films. The band gaps (E_g) of SnO_2 and TiO_2 are 3.86 eV and 3.52 eV, respectively. (d) UPS spectra at the cutoff (E_{cutoff}) energy regions of the mixed-cation lead mixed-halide

perovskite film. The obtained Fermi level is 3.88 eV. (e) E_f-E_v for the perovskite film is 1.95 eV. The absorption edge of the perovskite film, and the E_g is calculated to be 1.61 eV. Note that $\Phi = 21.21 - (E_{cutoff} - E_i)$, $VB = - | \Phi + (E_f - E_v) |$, $CB = VB + E_g$. Here Ei (onset energy) is calibrated to be 0 eV.

Table S1 Energy level related detailed parameters for SnO_2, TiO_2, TiO_2/SnO_2 and perovskite films.

Materials	E_{cutoff} (eV)	Φ (eV)	E_f-E_v (eV)	E_g (eV)	VB (eV)	CB (eV)
SnO_2	16.98	4.23	4.24	3.86	-8.47	-4.61
TiO_2	17.09	4.12	3.46	3.52	-7.58	-4.06
TiO_2/SnO_2	16.78	4.43	3.90	3.86	-8.33	-4.47
Perovskite	17.33	3.88	1.95	1.61	-5.83	-4.22

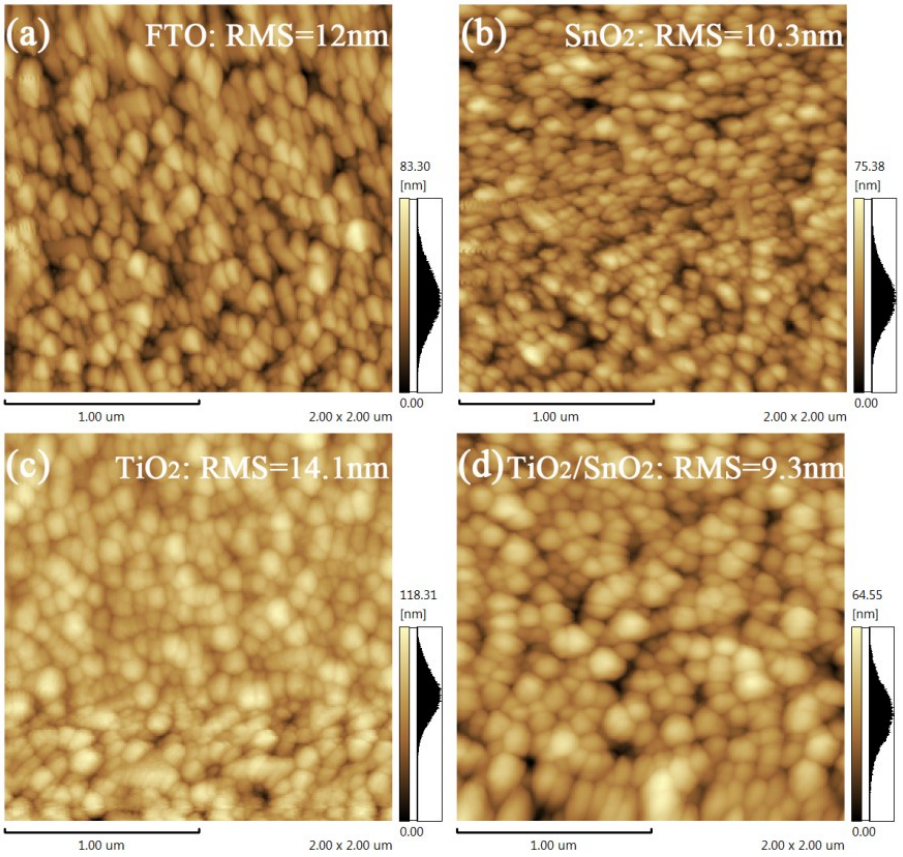

Fig. S2 1 × 1 μm^2 AFM scan of (a) bare FTO, (b) SnO_2, (c) TiO_2 and (d) TiO_2/SnO_2 films.

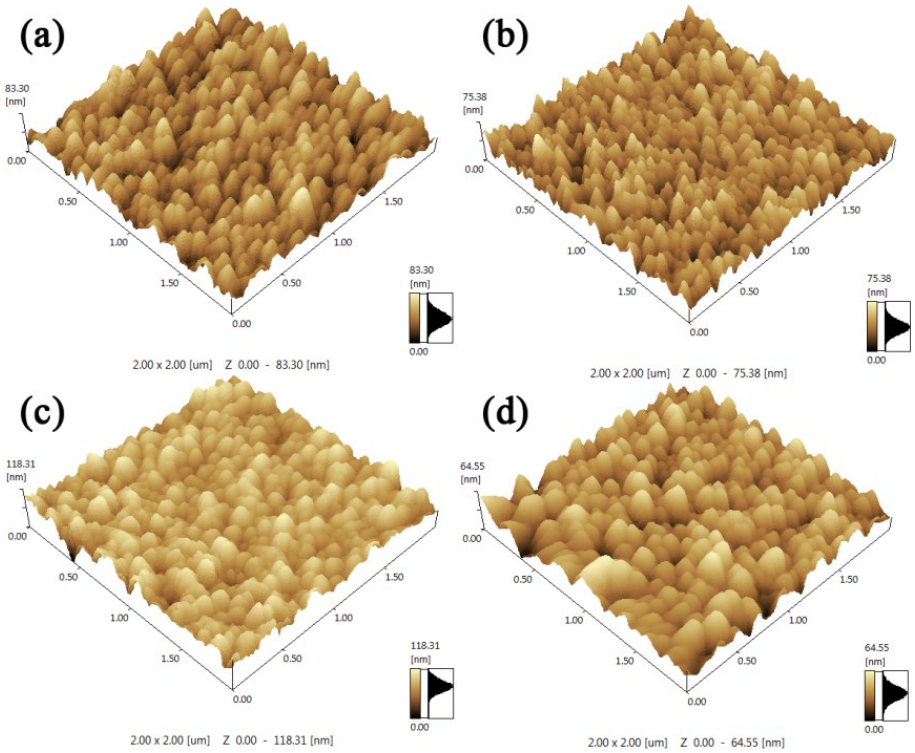

Fig. S3 3D AFM images of (a) bare FTO, (b) SnO_2, (c) TiO_2 and (d) TiO_2/SnO_2 films.

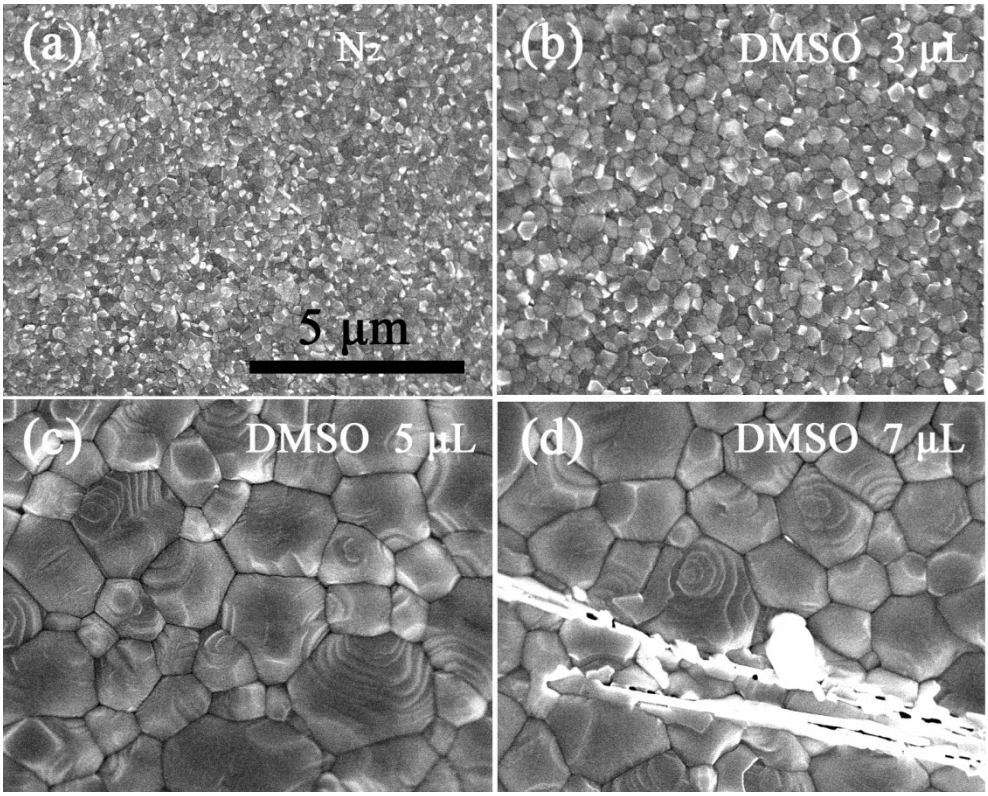

Fig. S4 Top-view SEM images of the perovskite layers prepared under different atmosphere.

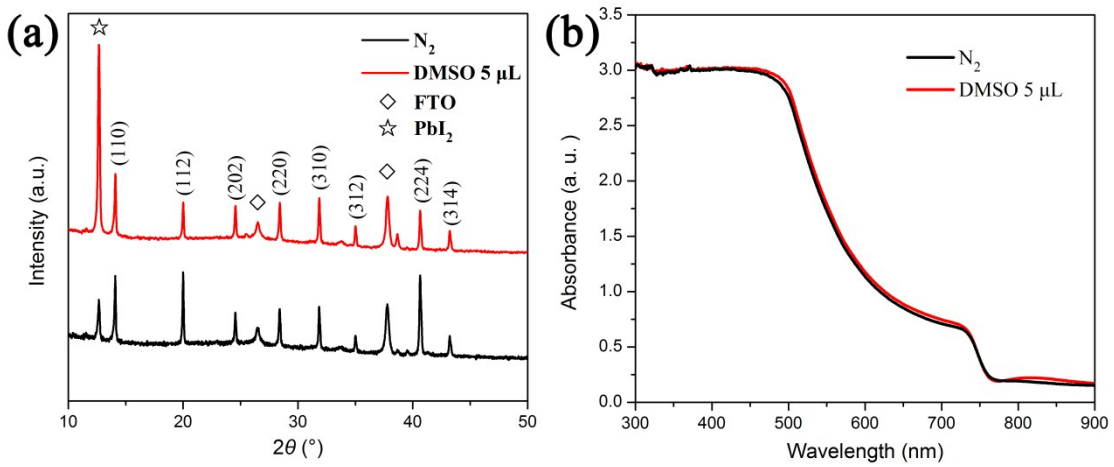

Fig. S5 (a) X-ray diffraction spectra and (b) ultraviolet to visible (UV-Vis) absorbance spectra of the perovskite layers annealed under different condition.

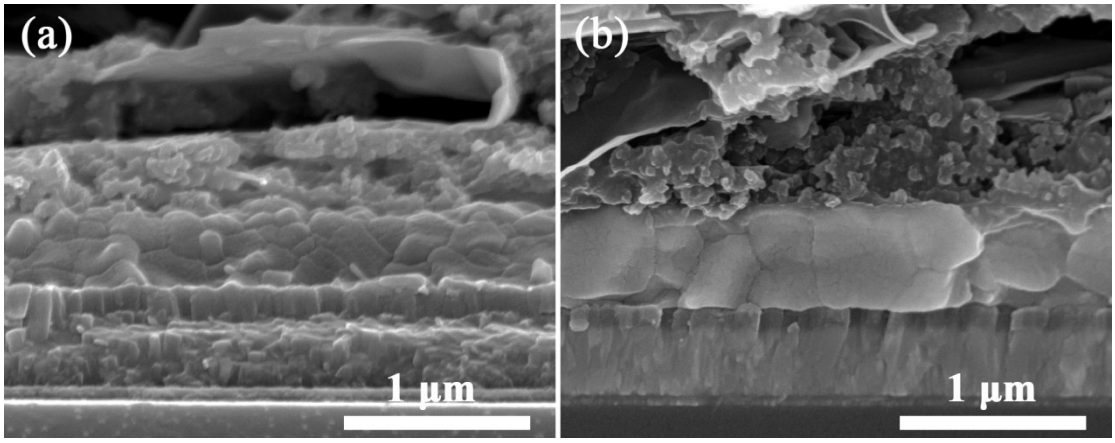

Fig. S6 Cross-sectional SEM images of the perovskite devices prepared under (a) N_2 and (b) DMSO vapor atmosphere.

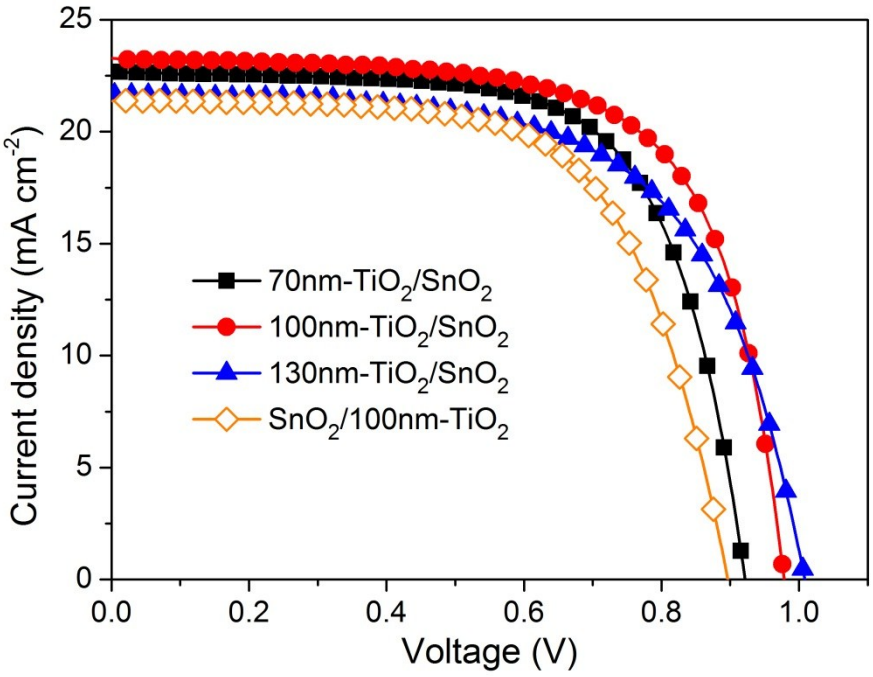

Fig. S7 *J-V* curves of the perovskite solar cells with different ETLs.

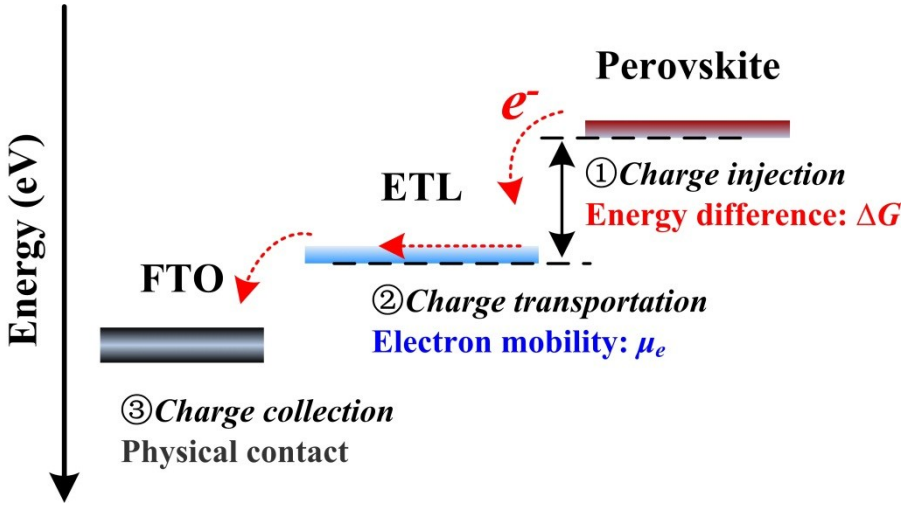

Fig. S8 Schematic illustration of the electron extraction in a n-i-p type planar solar cell. Electron extraction occurs from the perovskite to the FTO via injection, transportation, and collection.

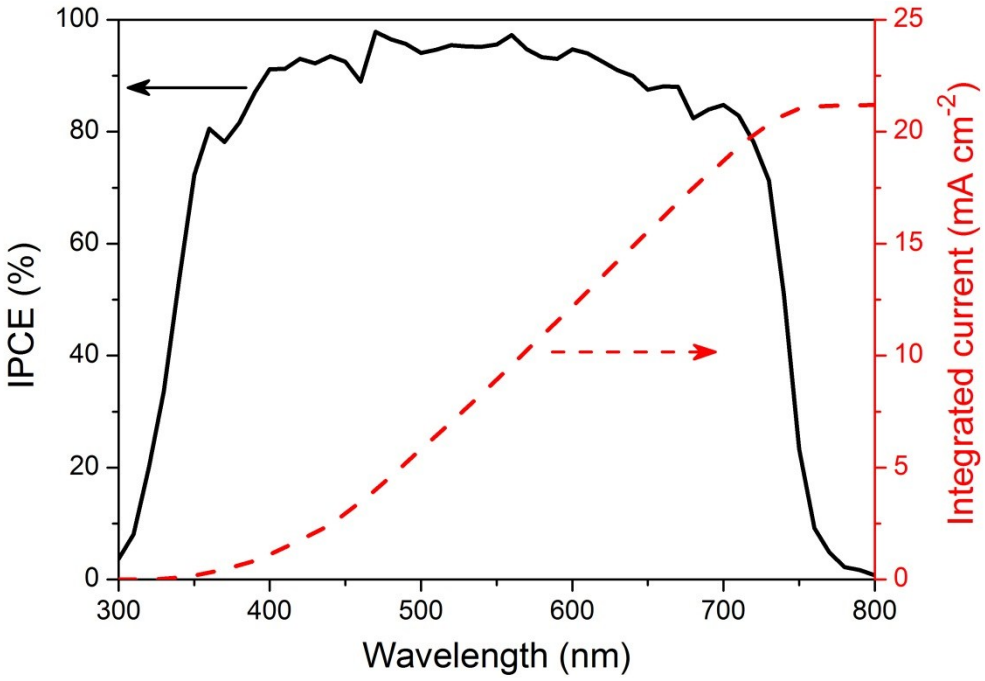

Fig. S9 IPCE of the PSCs and the integrated current calculated from the overlap integral of the IPCE spectra.

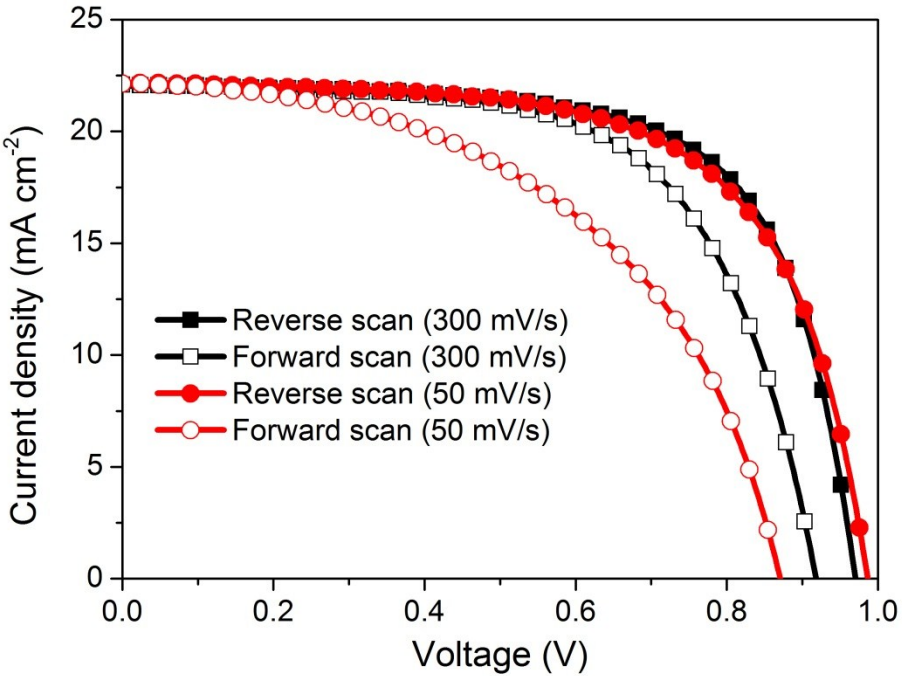

Fig. S10 *J-V* curves of the perovskite solar cell under reverse and forward voltage scanning.

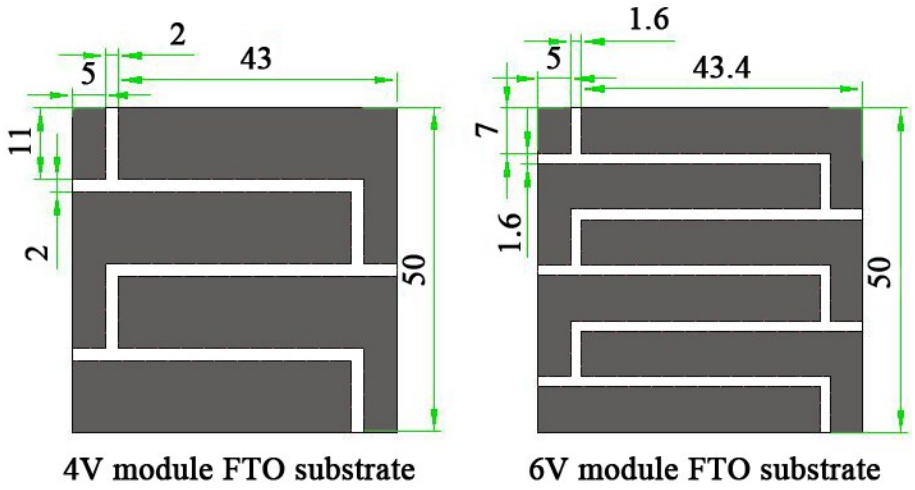

Fig. S11 The patterned FTO substrates for 4 V and 6 V modules (50 mm×50 mm).

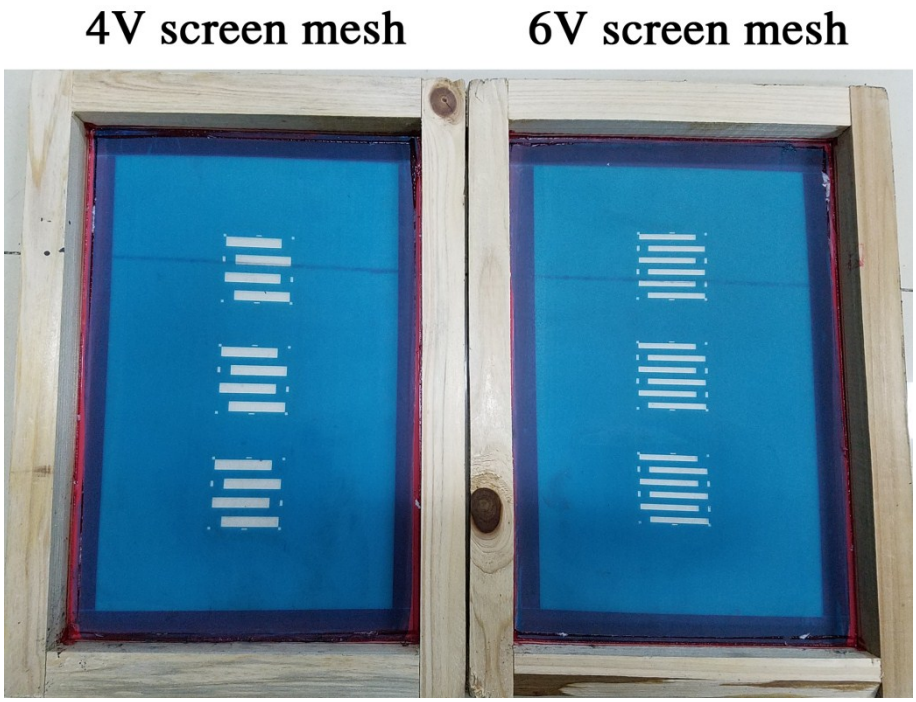

Fig. S12 Patterned screen meshes used to print the carbon electrode.